

Natural variability, radiative forcing and climate response in the recent hiatus reconciled

Markus Huber^{*} and Reto Knutti

Global mean surface warming over the past 15 years or so has been less than in earlier decades and than simulated by most climate models¹. Natural variability^{2–4}, a reduced radiative forcing^{5–7}, a smaller warming response to atmospheric carbon dioxide concentrations^{8,9} and coverage bias in the observations¹⁰ have been identified as potential causes. However, the explanations of the so-called ‘warming hiatus’ remain fragmented and the implications for long-term temperature projections are unclear. Here we estimate the contribution of internal variability associated with the El Niño/Southern Oscillation (ENSO) using segments of unforced climate model control simulations that match the observed climate variability. We find that ENSO variability analogous to that between 1997 or 1998 and 2012 leads to a cooling trend of about -0.06°C . In addition, updated solar and stratospheric aerosol forcings from observations explain a cooling trend of similar magnitude (-0.07°C). Accounting for these adjusted trends we show that a climate model of reduced complexity with a transient climate response of about 1.8°C is consistent with the temperature record of the past 15 years, as is the ensemble mean of the models in the Coupled Model Intercomparison Project Phase 5 (CMIP5). We conclude that there is little evidence for a systematic overestimation of the temperature response to increasing atmospheric CO_2 concentrations in the CMIP5 ensemble.

The recent slowdown in global-mean surface temperature since about 1998, often termed ‘hiatus’, continues to get a lot of attention. A number of factors have been proposed to contribute to the reduced observed warming or to the discrepancy between observed and simulated temperatures by climate models^{1–11}. However, a complete analysis integrating all of these aspects in a single coherent picture is lacking, and implications are rarely discussed. In terms of the magnitude of the Earth’s response to changes in past and future radiative forcing, it is critical to understand why global-mean warming has slowed down despite record emissions of CO_2 and whether the discrepancy between simulated and observed warming has implications for projections of future warming. If the discrepancy is due to natural variability or biases in non- CO_2 forcing, long-term future warming—dominated by CO_2 forcing—would not be significantly affected. A bias in the model response, however, would imply that warming projections would need to be revised.

An important role has been attributed to internal climate variability resulting from the ENSO and the Interdecadal Pacific Oscillation^{2,4}. The exceptional El Niño event in 1998 followed by several smaller La Niña events thereafter have reduced the anthropogenic warming trend during the past 15 years¹². A process

study showed that the observed strengthening of trade winds over the Pacific and the associated impact on subsurface temperatures and circulation can lead to a reduction of global temperature of $0.1\text{--}0.2^{\circ}\text{C}$ (ref. 13). Periods with reduced warming trends in climate models are also found to be associated with enhanced deep ocean heat uptake, suggesting a redistribution of energy rather than a lack of warming of the climate system^{3,14}.

Another factor leading to a slowed temperature increase during the past decade is a reduced radiative forcing¹¹. Several studies argued that the CMIP5 models overestimate recent warming trends because their prescribed input forcing did not account properly for increased stratospheric aerosols concentrations^{5–7} or the recent unusually low and long minimum of solar activity¹⁵. The representative concentration pathways (RCPs), with which almost all models are driven, mostly incorporated historical forcing estimates until 2005 and do not include these recent variations (Methods).

Reduced warming over the past 15 years might imply that equilibrium climate sensitivity (ECS) and transient climate response (TCR) (which characterize the equilibrium and transient temperature response to CO_2 , respectively) are smaller than previously thought, and overestimated in the CMIP5 models^{8,9,16,17}. However, the observed global temperature can be reproduced by various combinations of forcings and feedbacks¹⁸, making it difficult to disentangle the different contributions. In addition, even if the radiative forcing was known exactly, uncertainty in ocean heat uptake makes the estimation of climate sensitivity from the observed temperature change difficult. The temperature response per unit forcing further differs among forcing agents¹⁹ and models suggest that the TCR for non- CO_2 forcing such as aerosols and ozone is larger than to carbon dioxide²⁰. Finally, a bias in the observations owing to sparse data coverage, predominantly in the Arctic and around Antarctica¹⁰, presents an additional factor in the explanation of recent temperature trends.

Here we first present a new method to sample ‘variability analogues’, that is, segments in unforced control simulations of comprehensive (CMIP5) climate models to estimate the contribution of natural variability to the global temperature evolution during the past 15 years. Figure 1 shows the composite (average) of the variability analogue ensemble matching the 1997–2012 Niño3.4 Index (Methods), along with global surface air temperatures, sea surface temperatures (SSTs) and upper ocean temperatures (Fig. 1b–e). Segments of 23 out of 40 climate models are used (Supplementary Methods). Note that we combine selected segments of control runs, without additional forcing, prescribed SSTs or assuming empirical relationships between global-mean temperature and the Niño3.4 Index. Each segment thus represents

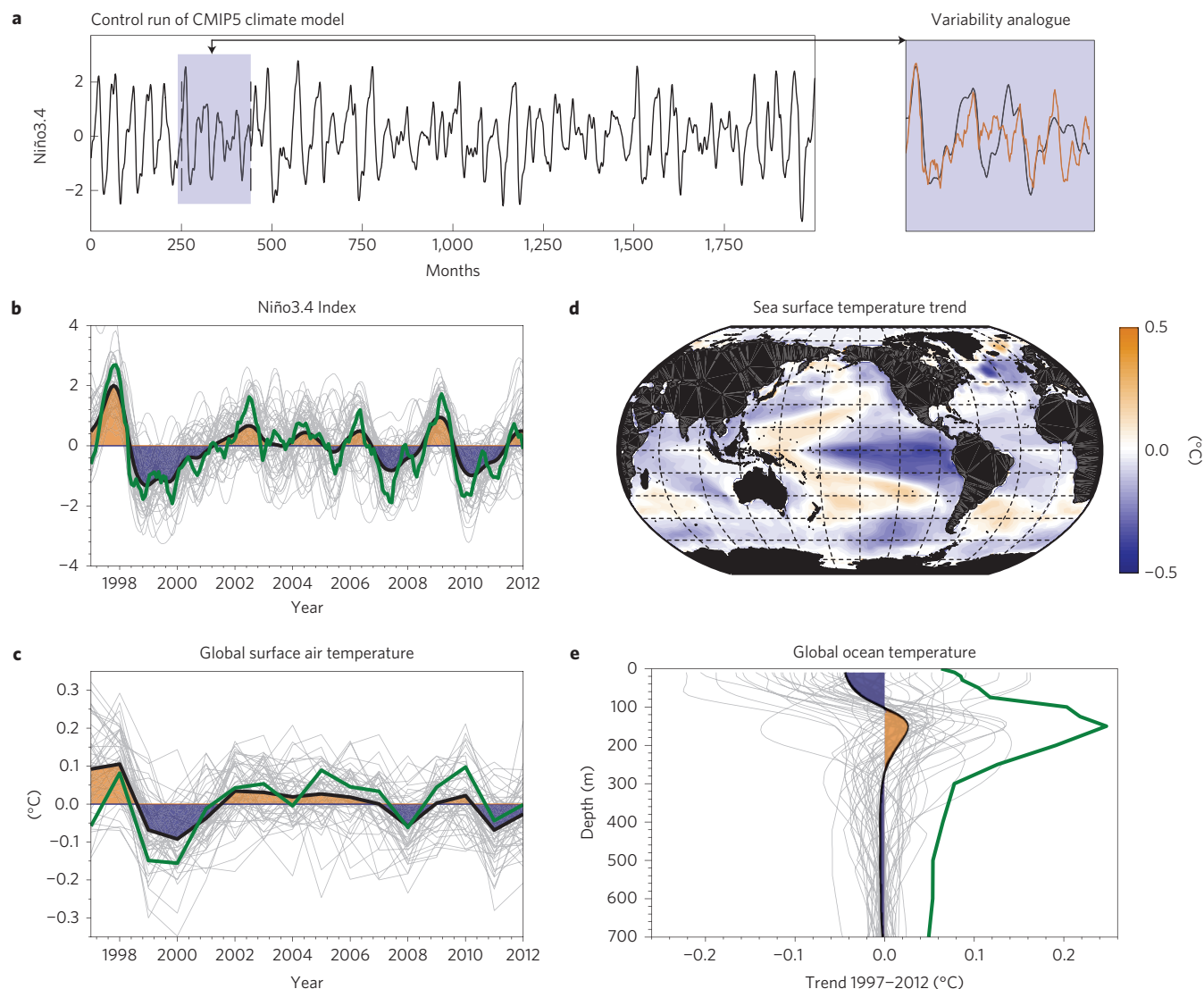


Figure 1 | Estimating the contribution of internal variability to recent temperature trends. **a**, Illustration of the method used to find segments in the unforced control simulation of a CMIP5 climate model that match the observed Niño3.4 Index (Methods). The right panel shows one such matching segment, which we refer to as a ‘variability analogue’. **b,c**, Evolution of the Niño3.4 Index and global surface air temperature between 1997–2012 for the variability analogue ensemble (grey lines) and observations (green). The ensemble-mean is denoted with the solid black line, illustrating positive (orange) and negative (blue) phases of the ENSO. **d,e**, Linear trend during 1997–2012 for SST (ensemble mean) and global averaged ocean temperatures in the model composite. Observations²⁹ are shown in green. Note that the long-term warming trend is by definition not present in the variability analogue in **e**.

an evolution of unforced climate variability in a CMIP5 model that accounts for partial details in the ocean and atmosphere warming pattern and is internally consistent from a dynamical as well as from an energy budget point of view. This contrasts with other methods that estimate the contribution of internal variability through simple regressions of an El Niño index to global temperature^{12,21}. The average of the segments we select can therefore be seen as a variability response pattern that emerges from all CMIP5 analogues available for the recent 15 years of observations.

The constructed composite matches the temporal evolution of the observations quite well, in particular the transition from an exceptional strong El Niño to a period with multiple La Niña phases afterwards. The realization of climate variability as captured by the analogues indicates a cooling trend of -0.06°C ($\pm 0.12^{\circ}\text{C}$, 1σ) since 1997 due to ENSO. As we use a relatively long period of about 15 years, the variability composite on average shows slightly less variance than the observations. The uncertainty in the estimated trend (Methods) is rather large, indicating that El Niño explains

only part of the variability in global temperature. Figure 1c also shows that the general evolution of inter-annual variability in the recent observations of global-mean temperature is captured by this method.

The composite analogue shows the familiar ENSO SST pattern with a strong cooling in the upwelling region of the equatorial Eastern Pacific (Fig. 1d). The signal of the variability analogues—defined by the average SST trend on each grid point divided by the standard deviation across the ensemble—is highest in this region, reaching values up to 0.9. The opposite horseshoe-like warming patterns flanking the cooling region is also evident. Below the surface, the composite shows on average a cooling in the top 100 m and enhanced warming in the 100–300 m depth range. The pattern shows a similar behaviour to the observed ocean warming profile, except that the variability analogue composite lacks the long-term warming that is present in the observations, because the former is derived from control run experiments. Consistent with recent arguments, the composite shows a positive anomaly in both the deep

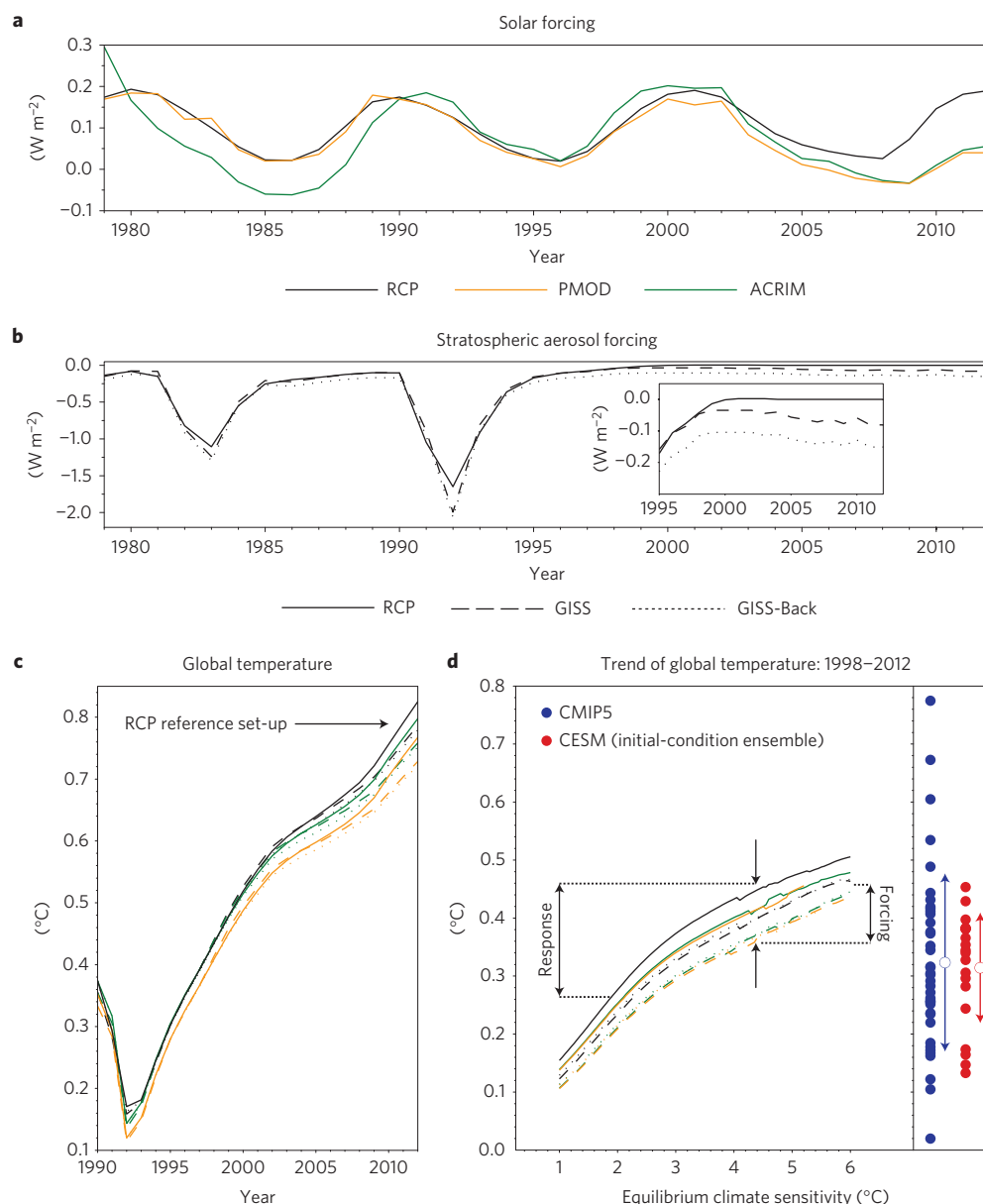


Figure 2 | Updated radiative forcings from solar irradiance and stratospheric aerosols and their impact on the recent temperature trends. **a,b**, Time series of solar radiative forcing (**a**) and stratospheric aerosol forcing (**b**) for the default RCP case (black) and revised data sets of total solar irradiance (coloured lines) and stratospheric aerosol optical depth (dashed and dotted lines; Methods). Note that in **a,b** historical estimates in the RCPs run through 2005, and the scenario starts from 2005 onwards. **c**, Evolution of global temperature derived with a climate model of intermediate complexity for the nine different forcing cases. The whole twentieth century is chosen as the reference period. **d**, Trends of global temperature during the 15-year period 1998–2012 for different climate sensitivities of the climate model and the nine forcing scenarios. The total forcing includes all anthropogenic and natural forcings of the RCP emission scenarios. Values of the CMIP5 climate models and a 20-member initial-condition ensemble of the Community Earth System Model (CESM) climate model²² are also shown. The arrows illustrate uncertainties associated with radiative forcing and climate response (black) as well as with the spread in the CMIP5 and CESM ensembles (blue and red, respectively).

and the total ocean heat uptake^{3,14} corresponding to surface cooling, but the magnitude is small and the spread across realizations is large.

We next quantify the effect of updated solar and stratospheric aerosol forcings (Fig. 2a,b) on the global-mean temperature change since 1990 using an Earth Model of Intermediate Complexity (EMIC) with an equilibrium climate sensitivity of 3 °C (corresponding to a transient climate response of 1.8 °C). This model has no internal variability and is thus ideal to study the effect of forcing and response. Compared with the default RCP forcing set, our updated forcing leads to a reduction in global temperature increase since 1998 of the order of -0.04 °C due to solar forcing and

-0.035 °C due to stratospheric aerosol, that is, -0.07 °C combined (Fig. 2d). Our estimate of the stratospheric aerosol contribution is slightly lower than previous estimates^{5,7}.

As climate sensitivity is a parameter in our EMIC, we can explore its effect on the temperature trend during the past 15 years (Fig. 2d). Updated forcings reduce the trend by -0.04 °C for a low sensitivity of 1 °C and -0.08 °C for a high sensitivity of 4.5 °C, reducing the default RCP trend between by 27% (ECS = 1 °C) to 18% (ECS = 4.5 °C). For the same period, the ranges of natural variability in a large initial-condition ensemble²² and in the CMIP5 multi-model ensemble (sampling both natural variability and response

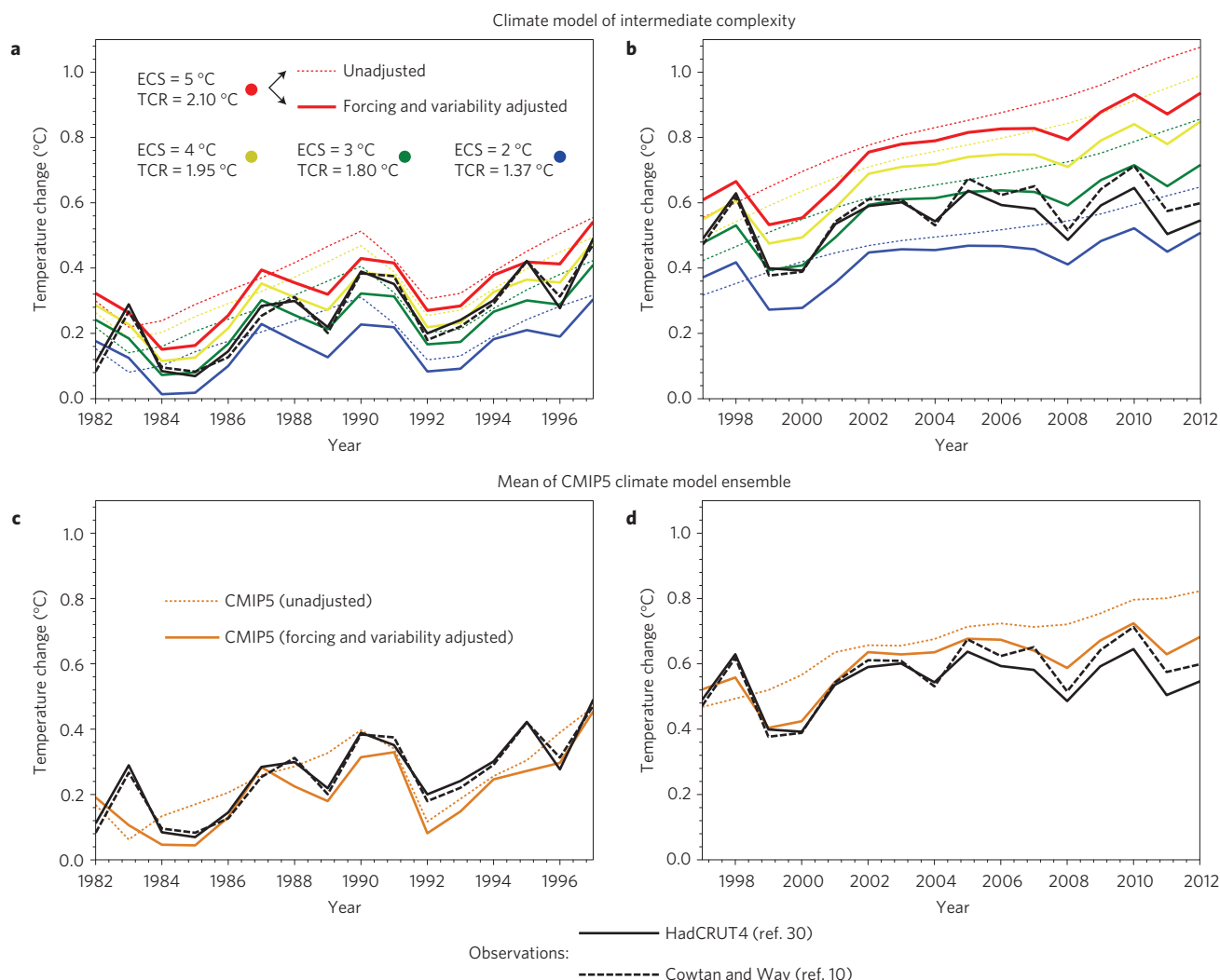


Figure 3 | Simulated global temperature adjusted with revised radiative forcings and the effect of internal variability. **a,b**, Changes of global temperature with respect to the whole twentieth century are shown for different climate sensitivity values computed with a climate model of reduced complexity (Methods). For each of the two periods shown, the simulations of the climate models are adjusted (coloured solid lines) with the effect of internal variability associated with the observed evolution of ENSO (Fig. 1) and revised radiative forcing (Fig. 2). **c,d**, Similar to **a,b**, but for the ensemble mean temperature change of the CMIP5 climate models. In all panels, observations from two data sets^{10,30} are shown in black, with the dashed case attempting to fill in missing data using observations other than those from the surface.

uncertainty resulting from the spread in climate sensitivity) are given for comparison in Fig. 2d.

Assuming linearity of the effect of the observed climate variability as captured by the variability analogue composite and the response of the climate system to revised solar and stratospheric aerosol radiative forcing, we can then impose these adjustments onto the simulated global temperature evolution simulated by the EMIC for different values of climate sensitivity (Fig. 3a) as well on the average of the CMIP5 climate models (Fig. 3b) for two 15-year-long periods. With a climate sensitivity of 3 °C and a transient climate response of 1.8 °C, the overall warming of the twentieth century as well as the year-by-year variations over the past decades are in good agreement. Adding the forcing corrections estimated with the EMIC and the natural variability component from the composite variability analogue to the CMIP5 multi-model mean gives an estimate of what the CMIP5 ensemble would have shown with updated forcings and a realization of variability that is consistent with observations. The resulting model mean agrees well with the coverage corrected observations¹⁰. Figure 3a demonstrates that a low climate sensitivity value is less consistent with the total

warming over the twentieth century when accounting for updated forcing and internal variability.

Our ‘variability analogue’ method presented here estimates that internal variability contributed a cooling trend of -0.06°C since 1997 to the observed global temperature trend on the basis of similarities in the evolution of tropical variability as measured by the Niño3.4 Index in observations and climate model control simulations. In contrast to other methods, our approach does not make use of additional forcing or prescribed SSTs. Despite being selected to match ENSO, each selected segment has a different realization of global surface air, sea surface and upper ocean temperature, in particular in the regions not strongly characterized by ENSO. Therefore, the composite over all segments mainly shows the ENSO-related contribution that is common to most segments across CMIP5 models (Methods). Moreover, it does not include further contributions by other variability patterns and mechanisms, for example, trends in high-latitude atmospheric circulation patterns. Variability indices other than the Niño3.4 Index could be chosen to pick alternative variability analogue segments.

The results presented here do not repeat the attribution of the observed warming to different causes²³. Nor do they strongly constrain ECS or TCR from the observed warming, which would require consideration of uncertainties in all forcings, feedbacks and heat uptake, and which is known to be difficult given all uncertainties¹⁸. Rather, they show what current climate models would have shown if some known systematic deficiencies in forcings had been considered, and if the models had a similar evolution of tropical variability. The results do not eliminate the possibility that some individual models may overestimate past or future warming²⁴, but they show that the temperature response to forcing in the CMIP5 ensemble as a whole is consistent with the observed warming and observationally constrained TCR estimates^{16,25}, in particular when the coverage bias is taken into account. As a consequence, recent claims of much lower climate sensitivities and future warming seem much less plausible. We show that the reduced warming and mismatch between models and observations since about 1997 or 1998 can, to a large extent, be explained by the combined effect of reduced forcing and natural variability, each of these components contributing about an equal amount. Further contributions to the warming hiatus by other variability mechanisms such as the Atlantic Multidecadal Oscillation cannot be excluded and uncertainties in radiative forcing, for example, in tropospheric aerosol forcing, persist and differ among models. However, we find little evidence for a biased model response of the CMIP5 ensemble as a whole and therefore expect long-term warming rates to increase again if variability and forcing were to shift back to values as in earlier periods.

Methods

We use monthly mean output of the Coupled Model Intercomparison Project (CMIP5) for surface air temperature (*tas*), sea surface temperature (*tos*) and ocean potential temperatures (*thetao*) from 40 climate models for the unforced control simulations (*piControl*) as well as the historical forcing scenario from the RCPs (ref. 26) during the twentieth century until year 2005, followed by the RCP8.5 scenario. The monthly fields were interpolated on a $2.5^\circ \times 2.5^\circ$ grid to compare the different climate models. A list of climate models with information regarding the length of the control simulation and the model drift is given in the Supplementary Methods.

For each control simulation of the CMIP5 climate models, we compute time series of the Niño3.4 Index by averaging monthly SST fields over the Niño3.4 region (5°S – 5°N and 120° – 170°W) and subtract the climatology over the entire control simulation. The index is normalized by the standard deviation over the control simulation and then compared with the observed Niño3.4 Index 1997–2012 as illustrated in Fig. 1a. The Niño3.4 observations are based on the NOAA (National Optical Astronomical Observatories) Optimum Interpolation Sea Surface Temperature V2 data set (obtained at www.cpc.ncep.noaa.gov/data/indices/sstoi.indices). We select those segments of the control simulation that match the evolution of the observations by applying a correlation criterion of $r=0.6$, leading to a set of 52 control segments matching the Niño3.4 observations. Only 2 of the 52 segments slightly overlap. We choose the threshold of $r=0.6$ to have a balance between the strength of correlation and the number of members selected into our variability analogue ensemble (see Supplementary Fig. 1 for a sensitivity analysis of the temperature trend of the variability ensemble to the correlation threshold).

The impact of a reduced radiative forcing on global mean temperatures is estimated with the Bern2.5D climate model of intermediate complexity (EMIC; ref. 27) driven with global-mean radiative forcing series from the RCP archive²⁶. In terms of solar forcing, the default RCP set-up is based on solar irradiance data by ref. 28 and repeats the 23rd solar cycle in the future, but implementations differ between models. The previous 23rd solar cycle lasted until about the year 2008, and updated records suggest that the minimum in 2009 was substantially lower than expected from a typical cycle¹⁵. This is not represented in the RCP set-up. We account for the prolonged solar cycle by using two observational data sets of total solar irradiance by the Active Cavity Radiometer Irradiance Monitor (ACRIM) and by the Physikalisch-Meteorologisches Observatorium Davos (PMOD). Both data sets are available at <http://www.acrim.com/TSI%20Monitoring.htm>. The two data sets show differences during their overlapping periods, and we derive radiative forcing time series for both data sets to account for the observational uncertainty. We also normalize the derived historical solar forcing to have an average of zero for the 22 years around 1750 (ref. 26).

The RCP forcing data set constitutes also the reference case in terms of stratospheric aerosol, which is based on previous volcanic stratospheric aerosol data used in the NASA (National Aeronautics and Space Administration) Goddard Institute for Space Studies (GISS) climate model up to the year 2001, followed by zero forcing to the year 2005 (ref. 26). Here, we use updated optical thickness time series (τ) from NASA GISS (accessed at http://data.giss.nasa.gov/modeler/strataer/tau.line_2012.12.txt) and convert them to radiative forcing with a conversion factor of $-23.5\text{ W m}^{-2}\tau^{-1}$, denoted by GISS in Fig. 2b. We further account for an additional negative radiative forcing during the period 1960–1990 of about -0.1 W m^{-2} suggested by observations⁵, denoted with by GISS-Back in Fig. 2b.

Received 6 March 2014; accepted 17 July 2014;
published online 17 August 2014

References

1. IPCC in *Climate Change 2013: The Physical Science Basis* (eds Stocker, T. F. et al.) (Cambridge Univ. Press, 2013).
2. Kosaka, Y. & Xie, S. P. Recent global-warming hiatus tied to equatorial Pacific surface cooling. *Nature* **501**, 403–407 (2013).
3. Meehl, G. A., Arblaster, J. M., Fasullo, J. T., Hu, A. X. & Trenberth, K. E. Model-based evidence of deep-ocean heat uptake during surface-temperature hiatus periods. *Nature Clim. Change* **1**, 360–364 (2011).
4. Meehl, G. A., Hu, A. X., Arblaster, J. M., Fasullo, J. & Trenberth, K. E. Externally forced and internally generated decadal climate variability associated with the interdecadal Pacific oscillation. *J. Clim.* **26**, 7298–7310 (2013).
5. Solomon, S. et al. The persistently variable 'Background' stratospheric aerosol layer and global climate change. *Science* **333**, 866–870 (2011).
6. Santer, B. D. et al. Volcanic contribution to decadal changes in tropospheric temperature. *Nature Geosci.* **7**, 185–189 (2014).
7. Fyfe, J. C., von Salzen, K., Cole, J. N. S., Gillett, N. P. & Vernier, J. P. Surface response to stratospheric aerosol changes in a coupled atmosphere-ocean model. *Geophys. Res. Lett.* **40**, 584–588 (2013).
8. Lewis, N. An objective Bayesian, improved approach for applying optimal fingerprint techniques to estimate climate sensitivity. *J. Clim.* **26**, 7414–7429 (2013).
9. Aldrin, M. et al. Bayesian estimation of climate sensitivity based on a simple climate model fitted to observations of hemispheric temperatures and global ocean heat content. *Environmetrics* **23**, 253–271 (2012).
10. Cowtan, K. & Way, R. G. Coverage bias in the HadCRUT4 temperature series and its impact on recent temperature trends. *Q. J. R. Meteorol. Soc.* <http://dx.doi.org/10.1002/qj.2297> (2014).
11. Schmidt, G. A., Shindell, D. T. & Tsigaridis, K. Reconciling warming trends. *Nature Geosci.* **7**, 158–160 (2014).
12. Rahmstorf, S., Foster, G. & Cazenave, A. Comparing climate projections to observations up to 2011. *Environ. Res. Lett.* **7**, 044035 (2012).
13. England, M. H. et al. Recent intensification of wind-driven circulation in the Pacific and the ongoing warming hiatus. *Nature Clim. Change* **4**, 222–227 (2014).
14. Trenberth, K. E. & Fasullo, J. T. An apparent hiatus in global warming? *Earth's Future* **1**, 19–32 (2013).
15. Frohlich, C. Total solar irradiance observations. *Surv. Geophys.* **33**, 453–473 (2012).
16. Otto, A. et al. Energy budget constraints on climate response. *Nature Geosci.* **6**, 415–416 (2013).
17. Gillett, N. P., Arora, V. K., Flato, G. M., Scinocca, J. F. & von Salzen, K. Improved constraints on 21st-century warming derived using 160 years of temperature observations. *Geophys. Res. Lett.* **39**, L01704 (2012).
18. Knutti, R. & Hegerl, G. C. The equilibrium sensitivity of the Earth's temperature to radiation changes. *Nature Geosci.* **1**, 735–743 (2008).
19. Hansen, J. et al. Efficacy of climate forcings. *J. Geophys. Res.* **110**, D18104 (2005).
20. Shindell, D. T. Inhomogeneous forcing and transient climate sensitivity. *Nature Clim. Change* **4**, 274–277 (2014).
21. Thompson, D. W. J., Wallace, J. M., Jones, P. D. & Kennedy, J. J. Identifying signatures of natural climate variability in time series of global-mean surface temperature: Methodology and insights. *J. Clim.* **22**, 6120–6141 (2009).
22. Fischer, E. M., Beyerle, U. & Knutti, R. Robust spatially aggregated projections of climate extremes. *Nature Clim. Change* **3**, 1033–1038 (2013).
23. Huber, M. & Knutti, R. Anthropogenic and natural warming inferred from changes in Earth's energy balance. *Nature Geosci.* **5**, 31–36 (2012).
24. Stott, P., Good, P., Jones, G., Gillett, N. & Hawkins, E. The upper end of climate model temperature projections is inconsistent with past warming. *Environ. Res. Lett.* **8**, 014024 (2013).

25. Collins, M. *et al.* in *Climate Change 2013: The Physical Science Basis* (eds Stocker, T. F. *et al.*) 1029–1136 (Cambridge Univ. Press, 2013).
26. Meinshausen, M. *et al.* The RCP greenhouse gas concentrations and their extensions from 1765 to 2300. *Climatic Change* **109**, 213–241 (2011).
27. Stocker, T. F., Wright, D. G. & Mysak, L. A. A zonally averaged, coupled ocean atmosphere model for paleoclimate studies. *J. Clim.* **5**, 773–797 (1992).
28. Lean, J. L. & Rind, D. H. How will Earth's surface temperature change in future decades? *Geophys. Res. Lett.* **36**, L15708 (2009).
29. Levitus, S. *et al.* World ocean heat content and thermosteric sea level change (0–2000 m), 1955–2010. *Geophys. Res. Lett.* **39**, L10603 (2012).
30. Morice, C. P., Kennedy, J. J., Rayner, N. A. & Jones, P. D. Quantifying uncertainties in global and regional temperature change using an ensemble of observational estimates: The HadCRUT4 data set. *J. Geophys. Res.* **117**, D08101 (2012).

Acknowledgements

We thank U. Beyerle for the technical support of the climate model and J. Sedlacek for helping with the CMIP5 data.

Author contributions

M.H. performed the climate model computations and analysis. Both authors designed the study and wrote the paper.

Additional information

Supplementary information is available in the [online version of the paper](#). Reprints and permissions information is available online at www.nature.com/reprints. Correspondence and requests for materials should be addressed to M.H.

Competing financial interests

The authors declare no competing financial interests.